Biodegradation (2011) 22:921–929
DOI 10.1007/s10532-010-9451-z

ORIGINAL PAPER

Bacterial Pu(V) reduction in the absence and presence of Fe(III)–NTA: modeling and experimental approach

Randhir P. Deo · Bruce E. Rittmann · Donald T. Reed

Received: 15 July 2010 / Accepted: 27 December 2010 / Published online: 14 January 2011

Abstract Plutonium (Pu), a key contaminant at sites associated with the manufacture of nuclear weapons and with nuclear-energy wastes, can be precipitated to "immobilized" plutonium phases in systems that promote bioreduction. Ferric iron (Fe^{3+}) is often present in contaminated sites, and its bioreduction to ferrous iron (Fe^{2+}) may be involved in the reduction of Pu to forms that precipitate. Alternately, Pu can be reduced directly by the bacteria. Besides Fe, contaminated sites often contain strong complexing ligands, such as nitrilotriacetic acid (NTA). We used biogeochemical modeling to interpret the experimental fate of Pu in the absence and presence of ferric iron (Fe^{3+}) and NTA under anaerobic conditions. In all cases, *Shewanella alga* BrY (*S. alga*) reduced Pu(V)(PuO_2^+) to Pu(III), and experimental evidence indicates that Pu(III) precipitated as $PuPO_{4(am)}$. In the absence of Fe^{3+} and NTA, reduction of PuO_2^+ was directly biotic, but modeling simulations support that PuO_2^+ reduction in the presence of Fe^{3+} and NTA was due to an abiotic stepwise reduction of PuO_2^+ to Pu^{4+}, followed by reduction of Pu^{4+} to Pu^{3+}, both through biogenically produced Fe^{2+}. This means that PuO_2^+ reduction was slowed by first having Fe^{3+} reduced to Fe^{2+}. Modeling results also show that the degree of $PuPO_{4(am)}$ precipitation depends on the NTA concentration. While precipitation out-competes complexation when NTA is present at the same or lower concentration than Pu, excess NTA can prevent precipitation of $PuPO_{4(am)}$.

Keywords Plutonium · *Shewanella alga* · Bacterial reduction · NTA · Iron · Bioreduction · Modeling

R. P. Deo (✉)
Chemistry Department, Division of Natural Sciences, College of Natural and Applied Sciences, University of Guam, Mangilao, Guam 96923, USA
e-mail: rdeo@uguam.uog.edu

B. E. Rittmann
Center for Environmental Biotechnology, Biodesign Institute, Arizona State University, Tempe, AZ 85287-5701, USA

D. T. Reed
Los Alamos National Laboratory, Environmental and Earth Sciences Division, Carlsbad Environmental Monitoring and Research Center, Carlsbad, NM 88220, USA

Introduction

The application of biotechnology for remediation of metals and radionuclides has been well documented (Banaszak et al. 1998, 1999a, b; Caccavo et al. 1992; Farrell et al. 1999; Gorby and Lovley 1992; Haas and Dichristina 2002; Liu et al. 2002; Lovley et al. 1993; Reed et al. 2010; Rittmann et al. 2002a; Songkasiri et al. 2002; Truex et al. 1997). Unlike for organic

contaminants, a bioremediation strategy for radionuclides and metals transforms them into phases that should render them immobile and recalcitrant (NRC 2000). This often proceeds via reduction of a radionuclide to an oxidation state that is less soluble.

The occurrence of plutonium (Pu) in the subsurface environment is a concern due to its long half-life (2.4×10^4 years) and toxicity (Neu et al. 2005). Under oxidizing conditions, the predominant forms of plutonium are $Pu(V)O_2^+$ and $Pu(VI)O_2^{2+}$, which form distinct inorganic/organic complexes when present as a contaminant in groundwater (Choppin 2003; Cleveland and Rees 1981). While PuO_2^+ (i.e., Pu(V)) does not form hydroxyl complexes until $pH > 8$ and should be very mobile under most subsurface conditions, PuO_2^{2+} (i.e., Pu(VI)) forms strong hydroxyl complexes and sorbs strongly to aquifer surfaces. However, Pu(VI) is easily reduced and not likely to persist in biologically active systems unless it undergoes irreversible aggregation and polymerization, which may stabilize it against reduction, leading to enhanced subsurface mobility and persistence in the oxidized form (Francis 2007; Reed et al. 2010).

The key to plutonium immobilization in the subsurface is its reduction to Pu(IV) and Pu(III) species. Of these two reduced oxidation states, Pu(IV) exhibits a lower solubility and a much higher tendency towards aggregation, polymer formation, and sorption. From this perspective, Pu(IV) is by far the preferred target oxidation state (Francis 2007; Reed et al. 2010).

Only a few papers have been published on bioreduction of Pu under anaerobic conditions: by *Bacillus polymyxa* and *circulans* (Rusin et al. 1994), *Geobacter metallireducens* GS15 and *Shewanella oneidensis* MR1 (Boukhalfa et al. 2007; Icopini et al. 2009), and *Clostridium* sp. (Francis et al. 2008). Furthermore, evidence of Pu reduction by abiotic mechanisms (Rai et al. 2002; Reed et al. 2006; von Gunten and Benes 1995) suggests that bioremediation strategies in subsurface environment require an understanding of coupled abiotic and biotic processes for accurate prediction of plutonium fate in complex subsurface environment (Banaszak et al. 1999a; Lovley 1993; Neu et al. 2002; Reed et al. 2010).

Our group published work on bioreduction of higher-valent uranium and plutonium (Reed et al. 2007), where part of that work investigated Pu(V) reduction in the absence and presence of Fe^{3+} and NTA. Specifically, we investigated the bioreduction of Pu(V) under anaerobic conditions with *Shewanella alga* BrY (a facultative metal-reducing bacterium (Caccavo et al. 1992, 1996) in the presence and absence of Fe^{3+}–NTA, an aqueous form of ferric iron. Although Pu(V) reduction occurred in both cases, reduction was significantly slower in the presence of iron. The suggested explanation was that Fe^{3+} was the preferred electron acceptor (over Pu(V)), but Fe^{2+}, once generated by bioreduction, caused concurrent abiotic reduction of Pu(V).

In this study, we use modeling analyses to understand the mechanisms governing the previously observed slow reduction of Pu(V) in the presence of iron (Reed et al. 2007). We also discuss new spectroscopic results that expand our ability to interpret the experimental findings.

Materials and methods

All methods to synthesize PuO_2^+; assay for Pu, Fe, lactate, and other organics; determine oxidation states of PuO_2^+ and Fe (Fe^{3+} and Fe^{2+}); grow *S. alga*; and carry out anaerobic experiments are the same as reported in Reed et al. (2007). For this work, we added spectroscopic analyses of the reduced Pu solid formed. The spectroscopic analysis was done using X-ray absorption near edge spectroscopy (XANES) with MR-CAT beamline at the Advanced Photon Source (APS) following the methods of Songkasiri et al. (2002).

Modeling

Background information on the biogeochemical model CCBATCH

Modeling was performed using the biogeochemical model CCBATCH (Rittmann et al. 2002b; VanBriesen and Rittmann 2000a, b), which was developed by our team to quantitatively link all the different types of reactions that control the fate of radionuclides and a range of other metals and organic co-contaminants. The basic structure of CCBATCH is described here, and then special features needed to use the model to

represent the experiments reported here are described. Certain details, such as parameter values, are reported as needed in "Results and discussion" section.

CCBATCH explicitly couples biological electron-donor and -acceptor consumptions to simultaneous chemical reactions in order to determine the effect of biological reactions on the fate of various components in the system. The original CCBATCH model (VanBriesen and Rittmann 1999, 2000a) couples microbially catalyzed reactions, which are kinetically controlled, with aqueous phase acid/base and complexation reactions, which are at thermodynamic equilibrium. Rittmann et al. (2002b) added a sub-model that links kinetically or equilibrium-controlled precipitation/dissolution to the microbial and aqueous-phase reactions. We used the equilibrium sub-model. CCBATCH was designed to describe batch reactions, such as those performed in this study. The microbial sub-model includes oxidation of an electron-donor substrate (e.g., lactate in our studies), synthesis and endogenous decay of biomass, stoichiometric utilization of an electron acceptor, and stoichiometric consumption or generation of inorganic carbon, ammonium–nitrogen, and acidic hydrogen. The equilibrium feature of the sub-model precipitates or dissolves just the amount of solid phase so that the aqueous phase speciation of the cation and anion match the solubility product (K_{sp}) for every time step. In general, precipitation consumes basic species, and the sub-model represents this through stoichiometric production of acidic hydrogen. Finally, CCBATCH computes pH based on changes in acidic hydrogen and solving a proton condition. To solve for equilibrium speciation, CCBATCH uses a Newton–Raphson technique that combines the aqueous-phase mass balances with mass action equilibrium expressions for all relevant acid/base and complexation reactions, and it can compute the equilibrium pH from the proton condition when the pH is not fixed.

Upgrading CCBATCH for anaerobic growth

To use CCBATCH to represent the experiments in which we saw slow reduction of Pu in the presence of Fe^{3+}–NTA, we first needed to upgrade the model to include anaerobic growth of *S. alga* using Fe^{3+}, not O_2, as the primary electron acceptor. One challenge is that Fe^{3+} complexes with many anionic species. We added complexes of Fe^{3+} with the common components of the medium, along with their respective equilibrium constants and stoichiometric mass balances; the complexes and formation constants are listed in Table 1a.

A second challenge is that the bioavailabilities of the various Fe^{3+} species are not known (Haas and Dichristina 2002). Since the pH of our experiments was buffered at neutral, pH has minimal effect on the relative concentrations of all Fe^{3+} species, and we could use total Fe^{3+} as the bioavailable form of Fe^{3+}. Table 1b summarizes the parameters used to describe Fe^{3+} bioreduction and biomass growth from it: $q_{lactate}$ = maximum specific rate of lactate utilization, $K_{a,Fe(III)}$ = electron acceptor concentration that gives half of the maximum growth rate, and b = first-order endogenous-decay rate. Should only one (or more than one) Fe^{3+} species be bioavailable, its concentration remains in a constant ratio with total Fe^{3+}; thus, the model would represent the experimental results equally well, but with the value of $q_{lactate}$ increased in proportion to the concentration ratio of total Fe^{3+} to the bioavailable species. The bioreduction of Fe^{3+} was not limited by lactate, since it was in excess.

The yield and stoichiometry for all components involved in Fe^{3+} bioreduction were based on the following overall reaction for lactate utilization coupled to biomass synthesis (Rittmann and McCarty 2001):

$$0.25CH_3CHOHCOO^- + 0.77Fe^{3+} + 0.0115NH_4^+ \rightarrow 0.0115C_5H_7O_2N + 0.25CH_3COO^- + 0.1925H_2CO_3 + 0.7815H^+ + 0.77Fe^{2+} \quad (1)$$

We also included in the model loss of *S. alga* cells due to cell decay (Rittmann and McCarty 2001; Hacherl and Kosson 2003):

$$0.05C_5H_7O_2N + Fe^{3+} \rightarrow 0.05NH_4^+ + 0.25H_2CO_3 + 0.95H^+ + Fe^{2+} \quad (2)$$

Biotic PuO_2^+ reduction

We added plutonium reactions into the model to represent reduction of PuO_2^+ in the presence and absence of Fe^{3+}–NTA for the experiments in Reed

Table 1 (a) Complexes and formation constants for Fe^{3+} complexes; (b) Kinetic parameters for Fe^{3+} and PuO_2^{+} reduction

Species	Log K	References
(a) Complexes and formation constants for Fe^{3+} complexes		
$Fe(Acetate)^{2+}$	4.24	Gustafsson (2009)
$Fe(Acetate)_2^{+}$	7.57	Gustafsson (2009)
$Fe(Acetate)_3$	9.5867	Gustafsson (2009)
$FeCl^{2+}$	1.48	Gustafsson (2009)
$FeH_2BO_3^{2+}$	−1.91	Gustafsson (2009)
$FeHNTA^{+}$	18.72	Gustafsson (2009)
$FeHPO_4^{+}$	22.285	Gustafsson (2009)
$FeH_2PO_4^{2+}$	23.85	Gustafsson (2009)
FeNTA	17.82	Gustafsson (2009)
$Fe(NTA)_2^{3-}$	25.92	Gustafsson (2009)
$Fe(OH)^{2+}$	−2.02	Gustafsson (2009)
$Fe(OH)_2^{+}$	−5.75	Gustafsson (2009)
$Fe(OH)_3$	−15	Gustafsson (2009)
$Fe(OH)_4^{-}$	−22.7	Gustafsson (2009)
$Fe_2(OH)_2^{4+}$	−2.894	Gustafsson (2009)
$Fe_3(OH)_4^{5+}$	−6.288	Gustafsson (2009)
$Fe(OH)CO_3$	−3.8	Smith et al. (2004)
$Fe(OH)NTA^{-}$	13.25	Gustafsson (2009)
$Fe(OH)_2NTA^{2-}$	5.24	Gustafsson (2009)
$Fe(OH)_3NTA^{3-}$	−6.12	Gustafsson (2009)
$Fe(SO_4)_2^{-}$	5.38	Gustafsson (2009)
$Fe(SO_4)^{+}$	4.25	Gustafsson (2009)

Parameter	Value	How estimated
(b) Kinetic parameters for Fe^{3+} and PuO_2^{+} reduction		
$q_{lactate}$	77.9 mole Lac. molcell^{-1} h^{-1}	Best fit to data
$K_{a,Fe(III)}$	4.3 mM	Best fit to data
b	0.024 day^{-1}	Hacherl and Kosson (2003)
k_1	0.892 M h^{-1}	Best fit to data
k_2	26.25 M^2 h^{-1}	Best fit to data
k_3	26.25 M^2 h^{-1}	Estimate

et al. (2007). In both the cases, we chose Pu^{3+} as the ultimate reduced form of plutonium based on X-ray absorption near edge spectroscopy (XANES) analysis of the solids formed at the end of the experiments. The potential for $Pu(V)O_2^{+}$ reduction to Pu^{3+} has been reported before under anaerobic conditions by metal-reducing bacteria: *Geobacter metallireducens* GS15 and *Shewanella oneidensis* MR1 (Boukhalfa et al. 2007), *Geobacter sulfurreducens* and *Shewanella oneidensis* (Renshaw et al. 2009), and *Clostridium* sp. (Francis et al. 2008).

Table 2 lists the formation constants of the major aqueous-phase species of $Pu(V)O_2^{+}$, $Pu(IV)^{4+}$, and $Pu(III)^{3+}$ included in the modeling. The last entry in Table 2 is the solubility product for $PuPO_{4(am)}$, the assumed solid phase for Pu^{3+}, which was modeled with the equilibrium feature of the precipitation/dissolution sub-model in CCBATCH (Rittmann et al. 2002b). The parameters that describe PuO_2^{+} bioreduction—k_1 = rate constant of biotic reduction without supporting growth, k_2 = abiotic reduction rate of PuO_2^{+} to Pu^{4+}, and k_3 = abiotic reduction rate of Pu^{4+} to Pu^{3+}—are given in Table 1b. Based on our observations and literature findings (Boukhalfa et al. 2007; Icopini et al. 2009), we assumed that biotic reduction of Pu(V) does not support growth of *S. alga*

Table 2 Formation constants for major Pu(V, IV, III) aqueous complexes at ionic strength = 0.1

Species	Log K	Ref.
$Pu(V)O_2CO_3^-$	5.12	Smith et al. (2004)
$Pu(V)O_2(CO_3)_2^{3-}$	6.5	Gustafsson (2009)
$Pu(V)O_2(CO_3)_3^{5-}$	5.5	Gustafsson (2009)
$Pu(V)O_2OH$	−9.7	Gustafsson (2009)
$Pu(V)O_2NTA$	6.75	Banaszak et al. (1999a)
$Pu(IV)(CO_3)_4^{4-}$	34.1	Gustafsson (2009)
$Pu(IV)(CO_3)_5^{6-}$	32.7	Gustafsson (2009)
$Pu(IV)(OH)_2^{2+}$	0.6	Gustafsson (2009)
$Pu(IV)(OH)_3^+$	−2.3	Gustafsson (2009)
$Pu(IV)(OH)_4$	−8.6	Gustafsson (2009)
$Pu(IV)NTA^+$	12.82	Banaszak et al. (1999a)
$Pu(IV)(SO_4)^{2+}$	5.5	Gustafsson (2009)
$Pu(III)(OH)_2^+$	−7	Gustafsson (2009)
$Pu(III)(CO_3)^+$	8.1	Gustafsson (2009)
$Pu(III)(CO_3)_2^-$	12.9	Gustafsson (2009)
$Pu(III)(CO_3)_3^{3-}$	15.4	Gustafsson (2009)
Pu(III)NTA	12.2	Gustafsson (2009)
$Pu(III)PO_{4(am)}$	Log $K_{sp} = -24.6$	Gustafsson (2009)

cells. The yield and stoichiometry for all components involved in PuO_2^+ bioreduction were based on the following overall reaction that coupled to lactate utilization:

$$0.25CH_3CHOHCOO^- + 0.5PuO_2^+ + H^+ \rightarrow 0.25CH_3COO^- + 0.25H_2CO_3 + 0.5Pu^{3+} + 0.5H_2O \quad (3)$$

Adding abiotic PuO_2^+ reduction

We represented the abiotic reductions of PuO_2^+ to Pu^{4+}(Eq. 4) and Pu^{4+} to Pu^{3+}(Eq. 5) by biologically produced Fe^{2+} with the following overall reaction:

$$PuO_2^+ + Fe^{2+} + 4H^+ \rightarrow Fe^{3+} + Pu^{4+} + 2H_2O \quad (4)$$

$$Pu^{4+} + Fe^{2+} \rightarrow Fe^{3+} + Pu^{3+} \quad (5)$$

For these reactions, we assumed first-order kinetics with respect to PuO_2^+, Pu^{4+} and Fe^{2+} concentrations:

$$\text{Rate} = k_2\left[PuO_2^+\right]\left[Fe^{2+}\right] \quad (6)$$

$$\text{Rate} = k_3\left[Pu^{4+}\right]\left[Fe^{2+}\right] \quad (7)$$

The values of k_2 and k_3 are listed in Table 1b.

Results and discussion

Figure 1 compares the experimental (Reed et al. 2007) and (new) modeling results for bioreduction of Fe^{3+}–NTA by *S. alga*. The modeling results for the transformations of all major components involved in bioreduction of Fe^{3+} accurately track the experimental results until ~12 h. This period included the parallel and stoichiometric utilization of lactate and reduction of Fe^{3+} to Fe^{2+}. *S. alga* showed a small amount of growth, which is clearly shown in the inset. After ~14 h, the model shows plateaus for all the components due to complete consumption of the limiting reactant, Fe^{3+}. The experiments do not show the total reduction of Fe^{3+} between 12 and 14 h. This can be attributed to the sudden loss of cell viability, as clearly shown in the inset. Thus, the modeling results up to 12 h represent well the transformations of all major components when *S. alga* was active. Furthermore, given the slow decay rate [i.e., 0.024 day^{-1} (Table 1)], we do not anticipate a significant loss of *S. alga* cells due to decay in the timeframe of the experiments conducted in this study.

Figure 2A compares model-calculated to experimental results (from Reed et al. 2007) for the bioreduction of PuO_2^+ to Pu^{3+} by *S. alga*. Although the experimental results for PuO_2^+ are sparse, modeling simulations show a good match to the experimental results past ~17 h. Also shown are model simulations for the stoichiometric oxidation of lactate to acetate and the formation of Pu^{3+}.

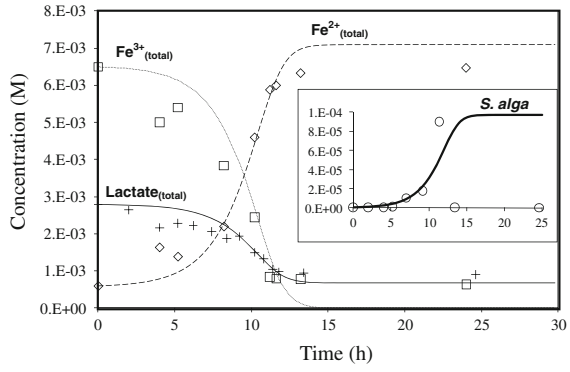

Fig. 1 Bioreduction of Fe^{3+}–NTA by *Shewanella alga*: comparison of modeling and experimental results (Reed et al. 2007). Model simulations are represented by *lines*, and experimental results are represented by *data points*

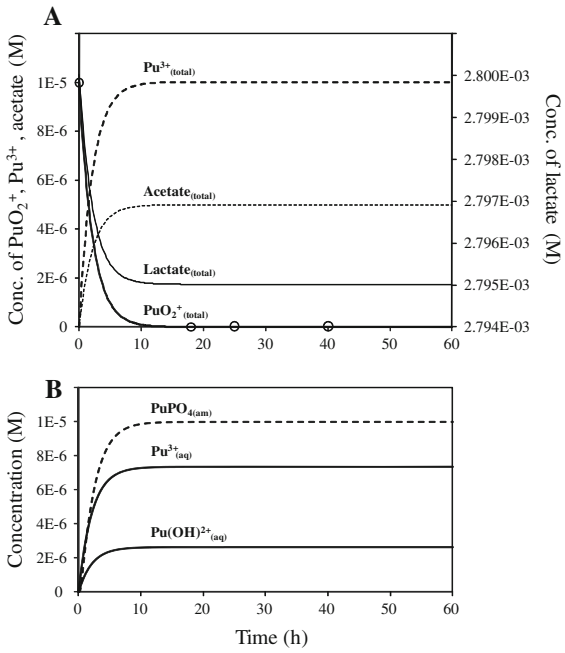

Fig. 2 **A** Comparison of model-calculated to experimental results (Reed et al. 2007) for the biotic reduction of PuO_2^+ by *Shewanella alga*. The *solid line* is the model simulation, and *open data points* are experimental results. Also shown are model simulations for consumption of lactate, and productions of acetate and Pu^{3+}. **B** Speciation of Pu^{3+} in the absence (*solid lines*) and presence (*dashed line*) of Pu^{3+} precipitate formation as $PuPO_{4(am)}$, but with no NTA

Modeling indicates that full bioreduction of 10 μM of PuO_2^+ required oxidation of ~0.18% of the initial lactate, which is practically not measureable.

Figure 2B shows the model-simulated speciation of Pu^{3+} in the absence (solid lines) or presence (dashed lines) of Pu^{3+} precipitate formation, i.e., $PuPO_{4(am)}$. NTA is not present in the medium. When the precipitation subroutine was "turned off" (solid lines for Pu species), the major aqueous Pu^{3+} species formed and their respective percentages are 26.4% for $Pu(OH)^{2+}_{(aq)}$ and 73.6% for $Pu^{3+}_{(aq)}$. The high percentage of free $Pu^{3+}_{(aq)}$ illustrates the lack of concentration and/or strength of anions in the medium to complex with all the Pu^{3+}. "Turning on" the precipitation subroutine (dashed line) precipitated all the Pu^{3+} as $PuPO_{4(am)}$. This means that Pu^{3+} complexation with anions present in the medium was not strong enough to keep Pu^{3+} in a soluble form when NTA was not present.

Given that the normal anions in the medium could not complex Pu^{3+} strongly enough to keep it in solution, we explored the effects of having the strong complexing ligand NTA present in the medium. Figure 3 shows modeling simulations for the effect of different concentrations of NTA on Pu^{3+} precipitation. At 10 μM NTA (equivalent to the initial PuO_2^+ concentration in the medium), all the Pu^{3+} precipitated, and the fate of Pu(III) was the same as Fig. 2B with precipitation turned on. In the presence of 1 mM NTA (100 fold more than the initial PuO_2^+ concentration), Pu^{3+} did not precipitate at all, because the strength of Pu^{3+}–NTA complex was great enough to completely out-compete Pu^{3+} precipitation. Decreasing the NTA concentration from 1 to 0.1 mM and 0.05 mM freed $Pu^{3+}_{(aq)}$, which combined with PO_4^{3-} to form $PuPO_{4(am)}$ to a greater extent with less NTA.

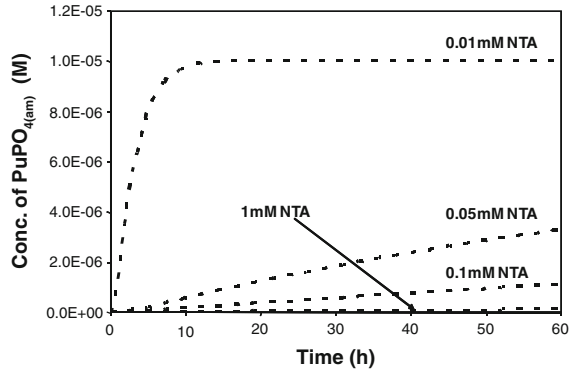

Fig. 3 Model simulations for the effect of different concentrations of NTA on Pu^{3+} precipitate formation as $PuPO_{4(am)}$

Next, we tested our hypothesis for the slowed reduction of plutonium in the presence of Fe^{3+}–NTA: i.e., preferential reduction of Fe^{3+} followed by abiotic reduction of PuO_2^+ by the biogenic Fe^{2+}. We previously showed experimental evidence to support abiotic reduction of PuO_2^+ by biogenically produced Fe^{2+} (Reed et al. 2007). Figure 4A compares the model-calculated and experimental results for the bioreduction of PuO_2^+ by *S. alga* in the presence of Fe^{3+}–NTA. It also shows the buildup of Fe^{2+} upon biotic reduction of Fe^{3+}. The modeling simulation provide a good fit to the experimental results of the previous experiments (Reed et al. 2007), supporting our hypothesis that the reduction of PuO_2^+ in the presence of Fe^{3+} was slowed (~40 h, compared to <17 h for direct biotic reduction of PuO_2^+—Fig. 2A) by preferential reduction of Fe^{3+}, but that the produced Fe^{2+} (Figs. 1, 4A—inset) abiotically reduced PuO_2^+ to Pu^{4+} and then to

Pu^{3+}. Although abiotic reduction of Pu by Fe^{2+} was reported for $Pu(IV)O_{2(am)}$ (Rai et al. 2002) and Pu(VI) (Reed et al. 2006), we are the first to describe stepwise reductions of PuO_2^+ to Pu^{4+} and to Pu^{3+} and to quantify how it is coupled with the biotic reactions that produce the Fe^{2+}.

Figure 4B shows the speciation of Pu^{3+} in the absence (i) or presence (ii) of $PuPO_{4(am)}$ precipitation. In both cases, almost all (99.8%) of Pu^{3+} was Pu^{3+}–$NTA_{(aq)}$, which can be attributed to the strength of Pu^{3+}–NTA complex (e.g., Fig. 3). The remaining ~0.2% of Pu^{3+} was speciated as free $Pu^{3+}{}_{(aq)}$ and $Pu(OH)^{2+}{}_{(aq)}$, with an additional ~0.07% of $PuPO_{4(am)}$ formed only when the precipitation subroutine was turned on (ii). In contrast to the no-NTA results of Fig. 2B, the presence of NTA in the medium kept Pu^{3+} in a soluble form in Fig. 4B.

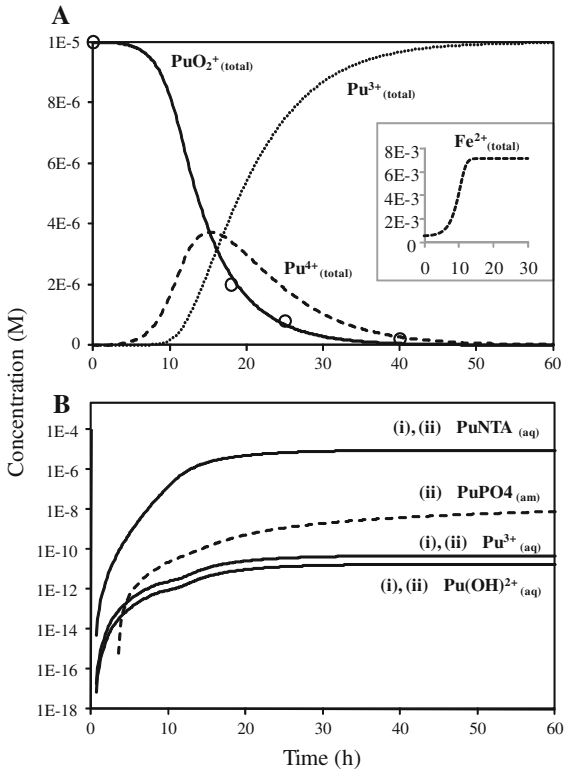

Fig. 4 **A** Comparison of model-calculated and experimental results (Reed et al. 2007) for abiotic (in the presence of Fe^{3+}–NTA) reductions of PuO_2^+ to Pu^{4+}, followed by Pu^{4+} to Pu^{3+}, by produced Fe^{2+}. Model simulations are represented by *lines*, and experimental results are represented by *data points*. Also shown is the buildup of produced Fe^{2+} upon preferred biotic reduction of Fe^{3+} (*inset*). **B** Speciation of Pu^{3+} in the absence (*i*) and presence (*ii*) of Pu^{3+} precipitate formation as $PuPO_{4(am)}$

While the desired end product is a bio-precipitated plutonium phase, modeling interpretation of experimental results shows that strong complexing ligands form soluble plutonium phases that are mobile, thus defeating an immobilization strategy. Such undesired reduced products were also observed upon reductions of uranium—forming U(IV)–citric acid complex (Francis and Dodge 2008)—and plutonium—forming Pu^{3+}–EDTA (Boukhalfa et al. 2007) and Pu^{3+}–NTA (Rusin et al. 1994).

Conclusions

We used biogeochemical modeling of experimental results in Reed et al. (2007) to advance our understanding of the fate of Pu in the absence and presence of Fe^{3+}–NTA under anaerobic conditions. In all experiments, *S. alga* reduced PuO_2^+ to Pu^{3+}, and evidence indicates that the Pu^{3+} could be precipitated as $PuPO_{4(am)}$. Modeling simulations support that reduction in the absence of Fe^{3+}–NTA was from direct biotic PuO_2^+ reduction, but that PuO_2^+ reduction in the presence of Fe^{3+}–NTA was due to an abiotic reduction reaction by biogenically produced Fe^{2+}. These results explain that PuO_2^+ reduction was slowed in the presence of Fe^{3+}–NTA because the bacteria preferentially reduced Fe^{3+} to Fe^{2+}, which then abiotically reduced Pu(V) stepwise to Pu(IV) and then to Pu(III). Modeling results also show that the degree of $PuPO_{4(am)}$ precipitation depended on the concentration of the strong complexing ligand NTA. While precipitation out-competed complexation when NTA had an equimolar or smaller concentration compared to Pu, an excess of NTA could completely prevent precipitation of $PuPO_{4(am)}$.

Acknowledgments The authors are grateful to Los Alamos National Laboratory for laboratory facilities. The research was supported, in part, by Environmental Remediation Sciences Program (ERSP) of the United States Department of Energy.

References

Banaszak JE, Reed DT, Rittmann BE (1998) Speciation-dependent toxicity of neptunium(V) toward *Chelatobacter heintzii*. Environ Sci Technol 32(8):1085–1091

Banaszak JE, Rittmann BE, Reed DT (1999a) Subsurface interactions of actinide species and microorganisms:

implications for the bioremediation of actinide-organic mixtures. J Radioanal Nucl Chem 241(2):385–435

Banaszak JE, Webb SM, Rittmann BE, Gaillard J-F, Reed DT (1999b) In: Wronkiewicz DJ, Lee JH (eds) Scientific basis for nuclear waste management XXII, vol 556, pp 1141–1149

Boukhalfa H, Icopini GA, Reilly SD, Neu MP (2007) Plutonium(IV) reduction by the metal-reducing bacteria *Geobacter metallireducens* GS15 and *Shewanella oneidensis* MR1. Appl Environ Microbiol 73(18):5897–5903

Caccavo F, Blakemore RP, Lovley DR (1992) A hydrogen-oxidizing, Fe(III)-reducing microorganism from the Great Bay estuary, New Hamshire. Appl Environ Microbiol 58(10):3211–3216

Caccavo F, Ramsing NB, Costerton JW (1996) Morphological and metabolic responses to starvation by the dissimilatory metal-reducing bacterium *Shewanella alga* BrY. Appl Environ Microbiol 62(12):4678–4682

Choppin GR (2003) Actinide speciation in the environment. Radiochim Acta 91:645–649

Cleveland JM, Rees TF (1981) Characterization of plutonium in Maxey Flats radioactive trench leachates. Science 212(4502):1506–1509

Farrell J, Bostick WD, Jarabek RJ, Fiedor JN (1999) Uranium removal from ground water using zero valent iron media. Ground Water 37(4):618–624

Francis AJ (2007) Microbial mobilization and immobilization of plutonium. J Alloy Compd 444:500–505

Francis AJ, Dodge CJ (2008) Bioreduction of uranium(VI) complexed with citric acid by *Clostridia* affects its structure and solubility. Environ Sci Technol 42(22): 8277–8282

Francis AJ, Dodge CJ, Gillow JB (2008) Reductive dissolution of Pu(IV) by *Clostridium* sp under anaerobic conditions. Environ Sci Technol 42(7):2355–2360

Gorby YA, Lovley DR (1992) Enzymatic uranium precipitation. Environ Sci Technol 26(1):205–207

Gustafsson JP (2009) Visual MINTEQ: version 2.61. KTH, Department of Land and Water Resources Engineering, Stockholm

Haas JR, Dichristina TJ (2002) Effects of Fe(III) chemical speciation on dissimilatory Fe(III) reduction by *Shewanella putrefaciens*. Environ Sci Technol 36(3):373–380

Hacherl EL, Kosson DS (2003) A kinetic model for bacterial Fe(III) oxide reduction in batch cultures. Water Resour Res 39(4):1098. doi:10.1029/2002WR001312

Icopini GA, Lack JG, Hersman LE, Neu MP, Boukhalfa H (2009) Plutonium(V/VI) reduction by the metal-reducing bacteria *Geobacter metallireducens* GS-15 and *Shewanella oneidensis* MR-1. Appl Environ Microbiol 75(11): 3641–3647

Liu CX, Gorby YA, Zachara JM, Fredrickson JK, Brown CF (2002) Reduction kinetics of Fe(III), Co(III), U(VI) Cr(VI) and Tc(VII) in cultures of dissimilatory metal-reducing bacteria. Biotechnol Bioeng 80(6):637–649

Lovley DR (1993) Dissimilatory metal reduction. Annu Rev Microbiol 47:263–290

Lovley DR, Widman PK, Woodward JC, Phillips EJP (1993) Reduction of uranium by cytochrome-C_3 of *Desulfovibrio vulgaris*. Appl Environ Microbiol 59(11):3572–3576

National Research Council (NRC) (2000) Natural attenuation for groundwater remediation. National Academy Press, Washington, DC

Neu MP, Ruggiero CE, Francis AJ (2002) In: Hoffman DC (ed) Advances in plutonium chemistry 1967–2000. University Research Alliance and American Nuclear Society, La Grange Park, pp 169–211

Neu MP, Icopini GA, Boukhalfa H (2005) Plutonium speciation affected by environmental bacteria. Radiochim Acta 93(11):705–714

Rai D, Gorby YA, Fredrickson JK, Moore DA, Yui M (2002) Reductive dissolution of PuO2(am): the effect of Fe(II) and hydroquinone. J Solut Chem 31(6):433–453

Reed DT, Lucchini JF, Aase SB, Kropf AJ (2006) Reduction of plutonium(VI) in brine under subsurface conditions. Radiochim Acta 94(9–11):591–597

Reed DT, Pepper SE, Richmann MK, Smith G, Deo R, Rittmann BE (2007) Subsurface bio-mediated reduction of higher-valent uranium and plutonium. J Alloy Compd 444:376–382

Reed DT, Deo RP, Rittmann BE (2010) Subsurface interactions of actinide species with microorganisms. In: Morss LR, Edelstein NM, Fuger J (eds) The chemistry of the actinide and transactinide elements, vol 6. Springer, New York, pp 3595–3663

Renshaw JC, Law N, Geissler A, Livens FR, Lloyd JR (2009) Impact of the Fe(III)-reducing bacteria *Geobacter sulfurreducens* and *Shewanella oneidensis* on the speciation of plutonium. Biogeochemistry 94(2):191–196

Rittmann BE, McCarty PL (2001) Environmental biotechnology: principles and applications. The McGraw-Hill Companies, Inc, New York

Rittmann BE, Banaszak JE, Reed DT (2002a) Reduction of Np(V) and precipitation of Np(IV) by an anaerobic microbial consortium. Biodegradation 13(5):329–342

Rittmann BE, Banaszak JE, VanBriesen JM, Reed DT (2002b) Mathematical modeling of precipitation and dissolution reactions in microbiological systems. Biodegradation 13(4):239–250

Rusin PA, Quintana L, Brainard JR, Strietelmeier BA, Tait CD, Ekberg SA, Palmer PD, Newton TW, Clark DL (1994) Solubilization of plutonium hydrous oxide by iron-reducing bacteria. Environ Sci Technol 28(9): 1686–1690

Smith RM, Martell AE, Motekaitis RJ (2004) NIST critically selected stability constants of metal complexes database, version 4.0. NIST: Standard Reference Data Program, Gaithersburg, MD

Songkasiri W, Reed DT, Rittmann BE (2002) Bio-sorption of neptunium(V) by *Pseudomonas fluorescens*. Radiochim Acta 90(9–11):785–789

Truex MJ, Peyton BM, Valentine NB, Gorby YA (1997) Kinetics of U(VI) reduction by a dissimilatory Fe(III)-reducing bacterium under non-growth conditions. Biotechnol Bioeng 55(3):490–496

VanBriesen JM, Rittmann BE (1999) Modeling speciation effects on biodegradation in mixed metal/chelate systems. Biodegradation 10(5):315–330

VanBriesen JM, Rittmann BE (2000a) Mathematical description of microbiological reactions involving intermediates. Biotechnol Bioeng 67(1):35–52

VanBriesen JM, Rittmann BE (2000b) Modeling biogeochemical interactions in co-contaminant systems. Abstr Pap Am Chem Soc 220:U338–U338

Von Gunten HR, Benes P (1995) Speciation of radionuclides in the environment. Radiochim Acta 69(1):1–29